

Parton evolution and saturation in deep inelastic scattering

J. Bartels^a

II. Institut für Theoretische Physik, Universität Hamburg, Luruper Chaussee 149, 22761 Hamburg, Germany

Received: 11 February 2005 /

Published online: 28 June 2005 – © Springer-Verlag / Società Italiana di Fisica 2005

Abstract. We review the evidence for saturation seen at HERA, and we discuss a few theoretical aspects of saturation in deep inelastic electron proton scattering.

PACS. 12.38.Bx, 12.38.-t, 12.38.Cy

1 Introduction

Measurements of deep inelastic structure functions at small x at HERA have stimulated novel ideas on parton dynamics in QCD, in particular the possible existence of states with high gluon density in electron–proton scattering (“saturation”) [1]. More recently, these ideas have been extended to heavy ion collisions [2], and arguments have been given that high gluon densities of the incoming heavy ions may initiate the formation of the searched-for quark gluon plasma. This talk summarizes the present evidence for saturation collected in deep inelastic electron–proton scattering (DIS) at HERA; I also address a few theoretical aspects of saturation in DIS.

In a reference frame where the proton has a large longitudinal momentum and the photon carries only a transverse momentum, the leading twist DGLAP description of deep inelastic scattering can be visualized in a cascade picture: the interaction of the virtual photon with the fast proton is through a single parton cascade which has its beginning long before the interaction with the photon. At small x , according to the linear DGLAP evolution equations, the cascade is mainly gluonic, and the cross section for this process becomes large, i.e. the probability for the photon of “finding a small- x ” gluon grows. Consequently, for sufficiently small values of x , also the probability of seeing a second, third, ... cascade (Fig. 1) starts to become non-negligible. The density of participating gluons grows, and interactions among these gluons come into play. The net result of these interactions is a weakening of the growth of the gluon density at small x . Once the density of gluons is high, the concept of “partons” is no longer appropriate, and the language of “strong classical fields” becomes more suitable.

This picture of the photon as “seeing” a field of high gluon density of the proton has also been named “color glass condensate” [2]. Here the term “condensate” hints at the high density, whereas “glass” refers to the life-time of

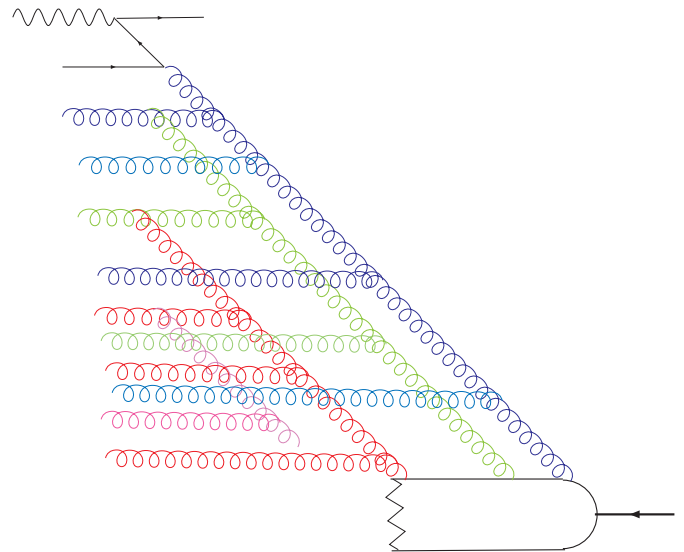


Fig. 1. Multi-cascade configurations at small x

the gluonic field which is much longer than the interaction time of the photon: the gluon field appears as a viscid medium.

An important feature of this saturation phenomenon is the appearance of a x -dependent momentum scale, $Q_s^2(x)$. The onset of saturation, as we have described, depends on the momentum scale Q^2 : the multi-cascade interactions start to become important at a certain x value which decreases with increasing Q^2 . This dependence can be inverted to define the saturation momentum scale $Q_s^2(x)$; calculations based upon the BFKL pomeron [3, 4] lead to the functional form

$$Q_s^2(x) = c \left(\frac{1}{x} \right)^\lambda, \quad (1)$$

where, typically, $\lambda \approx 0.3$. The constant scale parameter c , so far, cannot be calculated, but has to be determined

^a e-mail: bartels@mail.desy.de

from a (model-dependent) comparison with data. For Q^2 values larger than the saturation scale (1) the QCD parton model with the linear DGLAP evolution equations holds, whereas for smaller Q^2 values the saturation effects become visible. More elaborate calculations show that (1) is a too crude approximation: there are logarithmic corrections in front of the exponential, and also the exponent is a slightly more complicated function [5].

The experimental verification of saturation in DIS is an important task. If true, it means that partons with very small x originate from regions of high density and are probing subtle QCD dynamics. This would represent a step beyond the QCD-based parton picture, which deals with dilute partons only. As to practical applications, saturation has implications both for the analysis of heavy ion collisions at RHIC and of proton–proton scattering at the LHC. For the latter, saturation in DIS is expected to begin with the presence of multiple parton cascades; their measurement could be used to estimate, in proton–proton collisions, the effect of multiple partonic interactions and to understand the general structure of events. This clearly will help to control the background of new physics.

The HERA kinematic domain is not large enough, and the determination of the gluon density not precise enough to observe, as a signal of saturation, a flattening of the gluon density at fixed Q^2 and small x . So we have to look for other signals of saturation. The x -dependence of the saturation scale $Q_s^2(x)$ allows one to trace saturation not only at fixed Q^2 as a function of x , but also at fixed x as a function of Q^2 : this suggests to look, in DIS, for saturation effects also in the region of smaller Q^2 values where we expect to see the transition from the QCD parton picture to non-perturbative strong interactions. Clearly, in this region the use of perturbative arguments is less reliable. Nevertheless, this is the region where at HERA, so far, the strongest evidence for saturation comes from.

2 Evidence for saturation at HERA

In the following I review three different observations which, in my opinion, are indicative of saturation being present in the small- x and low- Q^2 region:

- (i) models based upon saturation ideas are successful in describing the deep inelastic proton structure function F_2 in the small- x region at low and at moderate Q^2 ;
- (ii) the observed geometric scaling of F_2 is a fundamental feature of saturation;
- (iii) the observed constant (with energy) ratio of DIS diffractive and DIS total cross sections has a natural explanation in saturation models.

Let me briefly comment on these observations.

The classical simple dipole saturation model (GBW) is due to Golec-Biernat and Wüsthoff [6]: with three parameters it successfully describes HERA data of F_2 in the low and intermediate Q^2 region; with a fourth parameter the description extends down to $Q^2 = 0$. Because of its simple analytic form it is straightforward to determine a saturation scale: the dipole cross section depends upon $r/R_s(x)$,

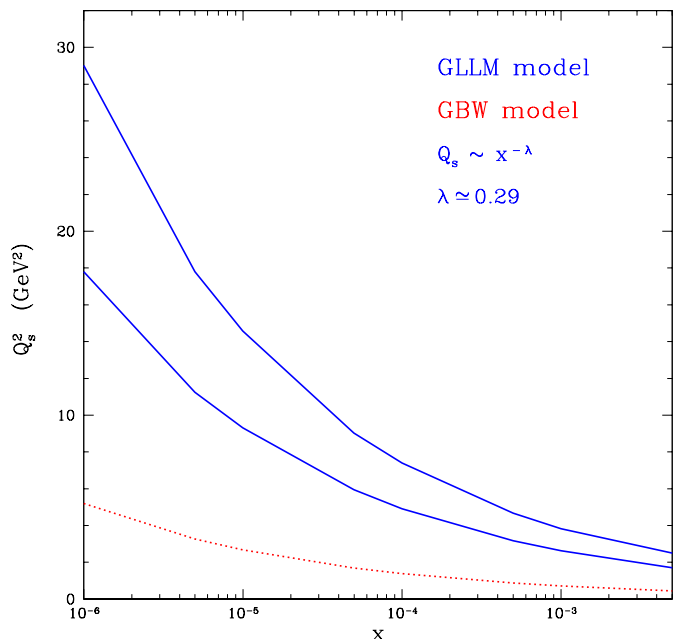


Fig. 2. Estimates of the saturation scales in two different models

where $R_s^2(x) = \frac{1}{Q_0^2} \left(\frac{x}{x_0}\right)^\lambda$. Inserting this into the dipole formula one arrives at the structure function F_2 which depends on the ratio $Q^2/Q_s^2(x)$ where $Q_s^2 = \frac{1}{R_s(x)}$, and, hence, predicts the observed property of geometric scaling [7]. In the x - Q^2 -plane (Fig. 2), the lower line is defined by $Q^2 = Q_s^2$, and it marks the transition region from pQCD to non-perturbative physics. Above this line the QCD parton model holds, and F_2 can be expanded in inverse powers of Q^2 (twist expansion [8]). Below, in the small- Q^2 region, a power series expansion in Q^2 applies. The transition between the two regions is not sharp, and it is not clear how far above the line corrections to DGLAP (higher twist corrections) could be significant. An improved version [9] of the GBW saturation model includes logarithmic scaling violations: this not only improves the quality of the fit to HERA data, but also extends the validity towards larger Q^2 values. An alternative saturation model [10], based upon an approximate solution of the non-linear Balitsky–Kovchegov equation, also describes the HERA data. As to the transition from pQCD to non-perturbative strong interactions, it leads to a somewhat different conclusion. The the upper two lines in Fig. 2¹ present, in the model of [10], two different definitions of the transition line, and the region between these lines can be interpreted as a “transition strip”. Compared with the GBW model, the limit of the linear evolution equations lies considerably higher, i.e. it is shifted towards larger Q^2 values. The discrepancy between the two models helps to illustrate the present uncertainty of where, in the x - Q^2 -plane, the applicability of the linear DGLAP evolution ends.

¹ I wish to thank M. Lublinsky for allowing me to use this figure.

It should be stressed that these saturation models have been constructed to describe the transition region at small x and moderate/small Q^2 where DGLAP is expected to require larger and larger corrections; their purpose is not to describe the region of large Q^2 and not too small x where the linear DGLAP evolution equations provide the adequate description. An important theoretical task, in particular for HERA physics, is the investigation of the matching of saturation models with the DGLAP fits. Saturation models in DIS are formulated within the color dipole picture which has been derived from QCD, so far, only in the leading- $\ln s$ approximation. In order to be able to compare with NLO DGLAP one needs, at least, the NLO analysis of the photon impact factor [11] and of the unintegrated parton distributions functions. Also, the analysis of low Q^2 data in terms of saturation models needs to be refined to include massive flavors, in particular charm. A critical discussion of the relation of saturation models and DGLAP has recently been given in [12].

As it has been said already, saturation leads to scaling properties of the dipole cross section and of the structure function F_2 . In particular,

$$F_2(x, Q^2) = F_2(Q^2/Q_s^2(x)). \quad (2)$$

This feature has clearly been seen in the data. Scaling has also been derived within the vector dominance model [13]; however, the energy dependence of the scaling momentum is different from the one of the saturation models.

DIS diffraction, most likely, provides the most sensitive test of saturation. One of the striking experimental results [14] is the energy dependence of the diffractive cross section, σ_{diff} : the ratio $\sigma_{\text{diff}}/\sigma_{\text{tot}}^{\gamma^*p}$ (at fixed region of diffractive masses) is nearly constant with energy. The saturation models, by a subtle interplay of the scales, reproduce this distinctive feature in a much more convincing manner than other models. It should, however, be noted that the saturation models for F_2 , as far as diffraction is concerned, are not completely satisfactory. Neither of them fully contains the diffractive $q\bar{q}$ and $q\bar{q}g$ final states (see below) which at HERA have been shown to contribute significantly.

The presented features provide evidence that saturation may be present in the small- x region at low/intermediate Q^2 values of F_2 and in DIS diffraction. Clearly, each feature by itself may allow for a different interpretation, and the comparison with saturation models cannot always claim to reach high precision. On the other hand, it is remarkable that the simple idea of the high gluon density allows one to explain different phenomena which, at first sight, look quite uncorrelated.

To collect further evidence we need to look for other – if possible: more direct – signals. This will be the task of the next few years. One direction of future research is the impact parameter (b) dependence of the dipole cross section. So far (i.e. in $\sigma_{\text{tot}}^{\gamma^*p}$ and in the diffractive cross section at zero momentum transfer t) we have been dealing with b -integrated cross sections; but HERA data also include the dependence on t : studies of b -dependent dipole cross sections have been started [15] and need further attention.

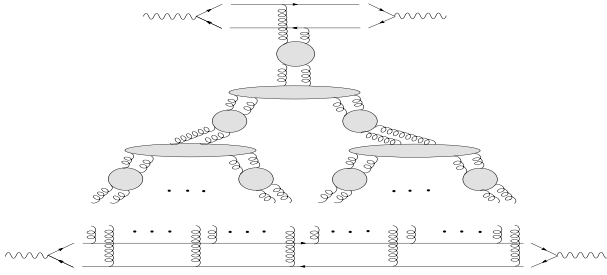
Another route of looking for signals of saturation is the investigation of multi-parton chains. As we have mentioned before, large gluon densities start with the formation and the interaction of multiple chains of partons. One should therefore look for signals of these multiple interactions. Direct evidence for the presence of double chains follows from the presence of DIS diffraction: the hard part of the diffractive final states cannot be counted as being part of the initial conditions to the (leading twist) parton densities. A recent analysis [16] has been based upon this fact, and it shows that the proper account of this fraction of diffractive data may lead to changes in the global fit of parton densities in the low Q^2 region. The presence of multichain configurations also affects the cross sections for multijet final states in DIS. Such jet configurations can originate from both single chains or from multichain configurations. The conventional hard scattering formalism takes into account only single chains; a deviation from its predictions, therefore, might be indicative for the presence of multichains. Work in this direction is in progress.

3 Remarks on the Balitsky–Kovchegov equation in DIS

In the second part of this talk I would like to discuss a few issues of the theoretical background of saturation in deep inelastic scattering. The models which I have mentioned are inspired by QCD saturation, but do not yet pretend to be based upon systematic QCD calculations. Presently numerous investigations of saturation in QCD are being discussed, and I want to mention a few topics that are relevant for saturation in DIS.

An attractive theoretical tool for studying saturation in QCD is given by the Balitsky–Kovchegov (BK) equation [17], which represents a non-linear generalization of the LO BFKL equation and, when written in configuration space variables, has a particularly simple mathematical form. Since it seems natural to use this equation as a model in DIS, it is important to understand the content of this equation and to be able to compute necessary corrections. In the context of using the BK equation also for DIS diffraction, there is particular interest in the question of which part of the DIS diffractive cross section is included in the BK equation.

A good starting point of such an analysis is QCD reggeon field theory, derived from momentum space Feynman diagrams [18]. This approach allows one to compute NLO corrections and to keep a connection with hard scattering processes in QCD. Also, momentum space seems more suited to analyze final states, and analyze s -channel unitarity cuts of Feynman diagrams. In this field theory reggeized gluons play the role of the elementary fields, and the BFKL pomeron represents the bound states of two gluons. The $2 \rightarrow 4$ gluon vertex [19] describes the splitting of one pomeron into two pomerons, and invariance under Möbius transformations has been proven for both the BFKL kernel and for this $2 \rightarrow 4$ vertex. In order to obtain a scattering amplitude, the Green's function


Fig. 3. Fan diagram equation in QCD

couple to external impact factors; because of gauge invariance they have special properties which define the space of functions in which the reggeon field theory operators are acting.

In this language, a simple non-linear generalization of the BFKL equation is the fan diagram equation [20] which sums all fan-like diagrams, with all BFKL pomerons at the lower end of the fan structure coupling to a single common dipole (eikonal approximation) (Fig. 3); this equation can be used as a model for the scattering of a single small dipole (upper end) on another larger dipole (lower end).

The key element in this equation is the $2 \rightarrow 4$ gluon vertex [19] which has a rather simple structure:

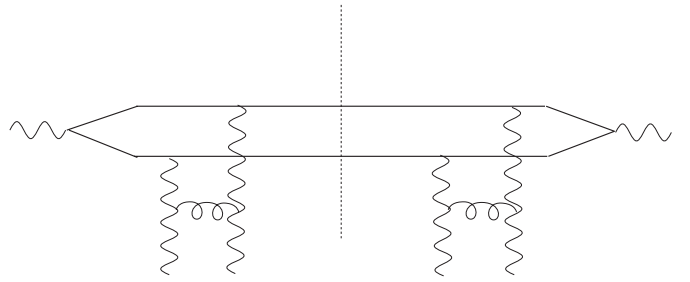
$$\begin{aligned} & \alpha_s^2 \mathcal{V}(q_1, q_2; k_1, k_2, k_3, k_4) \\ &= \frac{1}{(N_c^2 - 1)^2} (\delta_{a_1 a_2} \delta_{a_3 a_4} V(1234) + \delta_{a_1 a_3} \delta_{a_2 a_4} V(1324) \\ & \quad + \delta_{a_1 a_4} \delta_{a_2 a_3} V(1423)) , \end{aligned} \quad (3)$$

with the abbreviation $V(1234) = V(q_1, q_2; k_1, k_2, k_3, k_4)$. This function has good properties: it vanishes as any of the momenta $k_i \rightarrow 0$, and it is conformal invariant. Because of the apparent symmetry of the $2 \rightarrow 4$ vertex under the exchange of any pair of momenta and color labels, the AGK cutting rules are fulfilled. Within the reggeon field theory this vertex can also be used to compute pomeron loops (e.g. the self-energy of the pomeron Green's function).

Starting from this fan diagram equation in momentum space one can compute the Fourier transform and compare with the BK-equation for the dipole scattering amplitude N , which has the simple form

$$\begin{aligned} \frac{\partial}{\partial Y} N_{x,y} &= \bar{\alpha}_s \int \frac{d^2 z}{2\pi} \frac{|x-y|^2}{|x-z|^2 |y-z|^2} \\ & \quad \times (N_{x,z} + N_{y,z} - N_{x,y} - N_{x,z} N_{y,z}) \end{aligned} \quad (4)$$

(here x, y, \dots denote two-dimensional vectors in the transverse coordinate plane, and the subscripts in N_{xy} are the coordinates of the color dipole). One finds [21] that the Fourier transform of the $2 \rightarrow 4$ vertex is quite different from the kernel of the BK equation. However, making use of the Möbius properties of the reggeon field theory one can redefine the reggeon Green's functions and obtain a slightly simplified form of the kernel. Taking then also the limit $N_c \rightarrow \infty$, which selects the first term in (3) only, one finds that the Fourier transform of the $2 \rightarrow 4$ vertex


Fig. 4. Elastic scattering of a quark pair

coincides with the BK kernel [21]. Continuing along these lines it is also possible to compute corrections in $1/N_c^2$. From the point of view of the QCD reggeon field theory, the sum of fan diagrams represents a handy approximation. Apart from the coupling to the lower quark pair, the structure is classical, i.e. there are no real quantum corrections (closed pomeron loops). Eventually, however, one will have to go beyond this subset of diagrams of reggeized gluons and treat the interactions as a field theory in $2+1$ dimensions. In particular, closed pomeron loops [22] will have to be considered. Also NLO corrections to the $2 \rightarrow 4$ vertex should be computed, and higher interaction vertices (e.g. transitions $2 \rightarrow 6$) will appear. The reggeon field theory in momentum space provides a starting point for a systematic investigation, and Fourier transforming to configuration space allows one to make contact with the dipole picture.

When using the fan diagram equation or the BK equation for DIS cross sections, one first looks for saturation behavior of the dipole scattering amplitude N_{xy} , i.e. for properties that enter the total DIS cross section. This has been discussed at many other places and will not be repeated here. However, the observation of DIS diffractive final states at HERA suggests to ask for specific final states inside the total DIS cross section, in particular to trace diffraction inside the BK description of the total cross section. More specific, one has to address the question, how much diffraction of the upper dipole is included in this simple model of fan diagram equation; in other words, one has to investigate energy cuts through the fan diagrams. In particular, one is interested in the elastic intermediate state shown in Fig. 3. At first sight, since in Fig. 3 there is always a rapidity gap between the upper dipole and the first triple pomeron vertex underneath, it might seem as if there is no contribution from the elastic rescattering of the upper dipole. A closer inspection of the triple pomeron vertex [19], however, shows that this is not correct: in momentum space, the triple pomeron vertex contains “virtual pieces” which do not originate from real s -channel gluon production (quite in analogy to the BFKL vertex, which also consists of a “real” and a “virtual” contribution). These pieces can be traced back to parts of the diagrams shown in Fig. 3; from this one concludes that the triple pomeron vertex (3) does contain parts of the elastic intermediate $q\bar{q}$ state. Conversely, not the full $q\bar{q}$ state enters the triple pomeron vertex: the computation of the of the closed quark loop shows that there are other

pieces which belong to the reggeization of the gluon. Since the BK kernel (under the conditions described above) is the Fourier transform of V , it follows that also the BK equation has a part of elastic scattering being built in. It is not surprising that the question for the s -channel content of the BK equation cannot simply be answered by “yes” or “no”: both the fan diagram equation and the BK equation have been written for the elastic scattering of a dipole which, by the optical theorem, is related to the (completely inclusive) total cross section. The decomposition of the BK equation in terms of intermediate states may require another form.

In fact, it is instructive to re-organize the fan diagrams in such a way that one sees the elastic scattering explicitly [23]: in the large- N_c limit one can show that one can re-order the sum of Feynman diagrams in such a way that the coupling of two pomeron ladders to the $q\bar{q}$ dipole is separated from the remainder; as a result, one finds a new triple pomeron vertex (“diffractive vertex”), which is different from the one used in the BK equation: it turns out to coincide with the last two terms on (3). The Fourier transform to coordinate space has been computed in [21]; it has a fairly simple form:

$$-\bar{\alpha}_s \int \frac{d^2z}{2\pi} \frac{|x-y|^2}{|x-z|^2 |y-z|^2} \left[(N_{xz} + N_{zy} - N_{xy})^2 \right]. \quad (5)$$

The negative sign indicates that this kernel for the non-linear part again leads to the saturation for evolution in rapidity. It would be interesting to investigate solutions to the non-linear evolution equation (4), with the non-linear part of the kernel being replaced by (5).

In conclusion, for the further analysis of saturation in deep inelastic scattering it will be necessary to find theoretical descriptions of specific final states inside the high density system; this topic definitely requires further theoretical work.

4 Concluding remarks

We have reviewed a few phenomena in DIS at HERA which have a natural interpretation if saturation is assumed to be present at small- x and moderate Q^2 ; most of them are centered in the transition region where the analysis in terms of pQCD is expected to require substantial corrections. Each of the discussed phenomena, when considered separately, could possibly be explained by another and different model or mechanism; nevertheless it is remarkable that the simple idea of saturation provides a natural explanation of this variety of seemingly independent phenomena.

Theoretical studies of saturation in QCD are largely based upon the non-linear Balitsky–Kovchegov equation. This equation has been derived and investigated in coordinate space. For practical applications it is important to have the translation to momentum space. Further investigation of the role of saturation in deep inelastic scattering

will need to look into specific final states formed by the high density gluon system, in particular into the role of diffractive final states. The BK equation which has been designed for fully inclusive cross sections contains parts of the elastic $q\bar{q}$ intermediate state; it may, however, not be the best way to implement DIS diffraction into the description of saturation at HERA. Hence further theoretical work is needed to provide a realistic theory for HERA data.

References

1. L.V. Gibov, E.M. Levin, M.G. Ryskin, Phys. Rept. **100**, 1 (1983); A.H. Mueller, Jian-Wei Qiu, Nucl. Phys. B **268**, 427 (1986)
2. L.McLerran, R. Venugopalan, Phys. Rev. D **49**, 2233 (1994); D **50**, 2225 (1994)
3. L.N. Lipatov, Sov. J. Nucl. Phys. **23**, 338 (1976); V.S. Fadin, E.A. Kuraev, L.N. Lipatov, Phys. Lett. B **60**, 50 (1975); I.I. Balitsky, L.N. Lipatov, Sov. J. Nucl. Phys. **28**, 822 (1978); JETP Lett. **30**, 355 (1979)
4. E. Iancu, K. Itakura, L.McLerran, Nucl. Phys. A **708**, 327 (2002)
5. A.H. Mueller, D.N. Triantafyllopoulos, Nucl. Phys. B **640**, 331 (2002); S. Munier, R. Peschanski, Phys. Rev. Lett. **91**, 232001 (2003); Phys. Rev. D **69**, 034008 (2004)
6. K. Golec-Biernat, M. Wusthoff, Phys. Rev. D **59**, 014017 (1999); D **60**, 114023 (1999)
7. A.M. Stasto, K. Golec-Biernat, J. Kwiecinski, Phys. Rev. Lett. **86**, 596 (2001)
8. J. Bartels, K. Golec-Biernat, K. Peters, Eur. Phys. J. C **17**, 121 (2000)
9. J. Bartels, K. Golec-Biernat, H. Kowalski, Phys. Rev. D **66**, 014001 (2002)
10. E. Gotsman, E. Levin, M. Lublinsky, U. Maor, Eur. Phys. J. C **27**, 411 (2003)
11. J. Bartels, S. Gieseke, C.F. Qiao, Phys. Rev. D **63**, 056014 (2001) [Erratum D **65**, 079902 (2002)]; V.S. Fadin, D.Y. Ivanov, M.I. Kotsky, Atom. Nucl. **65**, 1513 (2002); J. Bartels, S. Gieseke, A. Kyrleis, Phys. Rev. D **65**, 014006 (2002); J. Bartels, D. Colferai, S. Gieseke, A. Kyrleis, Phys. Rev. D **66**, 094017 (2002); J. Bartels, A. Kyrleis, Phys. Rev. D **70**, 114003 (2004)
12. R.S. Thorne, CAVENDISH-HEP-05-01, hep-ph/0501124
13. D. Schildknecht, B. Surrow, M. Tentyukov, Mod. Phys. Lett. A **16**, 1829 (2001)
14. S. Chekanov et al, DESY 05-011, hep-ex/0501060
15. H. Kowalski, D. Teaney, Phys. Rev. D **68**, 114005 (2003)
16. A.D. Martin, M.G. Ryskin, G. Watt, Eur. Phys. J. C **37**, 285 (2004); hep-ph/0406225
17. I.I. Balitsky, Nucl. Phys. B **463**, 99 (1996); Phys. Rev. D **60**, 014020 (1999); Y.V. Kovchegov, Phys. Rev. D **60**, 034008 (1999); Phys. Rev. D **61**, 074018 (2000)
18. L.N. Lipatov, Nucl. Phys. B **452**, 369 (1995); J. Bartels, C. Ewerz, JHEP **9909**, 026 (1999)
19. J. Bartels, M. Wusthoff, Z. Phys. C **66**, 157 (1995); M.A. Braun, G.P. Vacca, Eur. Phys. J. C **6**, 147 (1999)
20. L.V. Gibov, E.M. Levin, M.G. Ryskin, Phys. Rept. **100** (1983)
21. J. Bartels, L.N. Lipatov, G.P. Vacca, hep-ph/0404110
22. J. Bartels, M.G. Ryskin, G.P. Vacca, Eur. Phys. J. C **27**, 101 (2003)
23. J. Bartels, M.A. Braun, G.P. Vacca, hep-ph/0412218